

## Supplementary Information

### **Interfacial compatibility critically controls Ru/TiO<sub>2</sub> metal-support interaction modes in CO<sub>2</sub> hydrogenation**

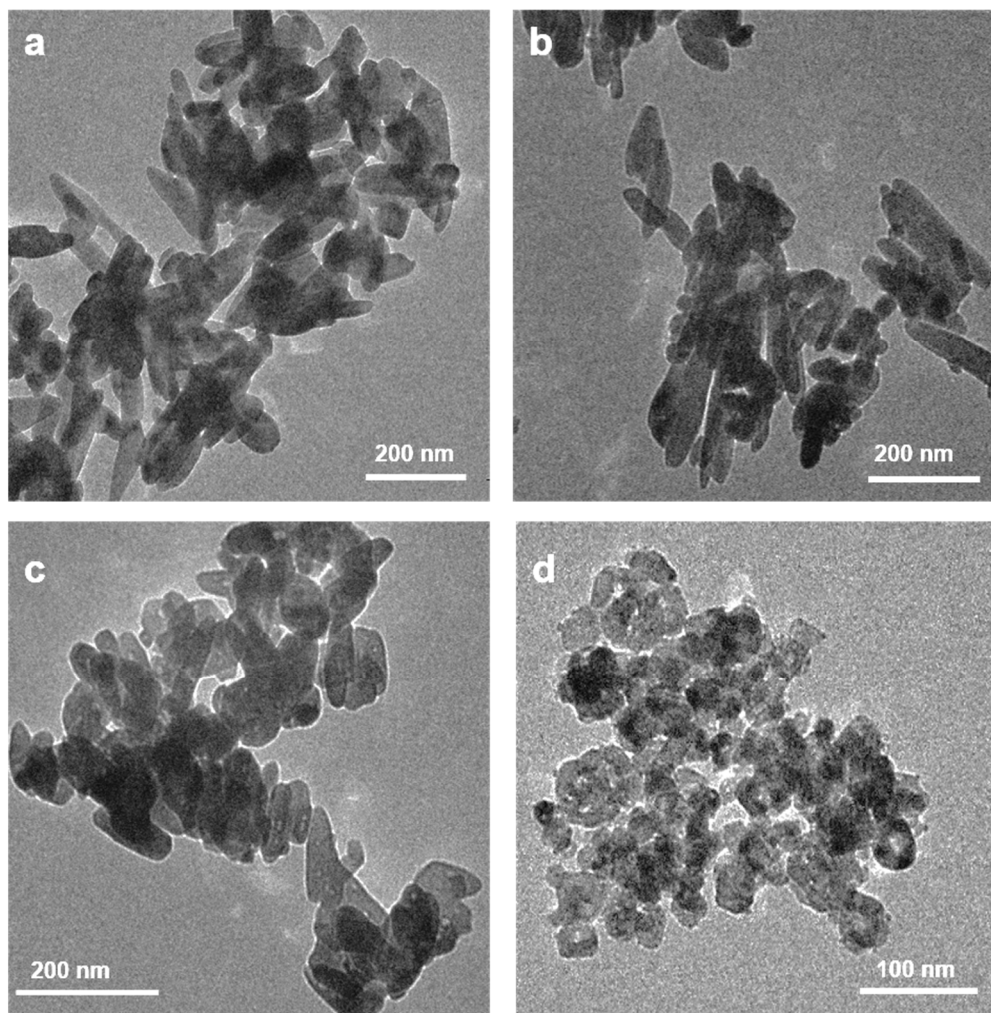
Jun Zhou<sup>1+</sup>, Zhe Gao<sup>2+</sup>, Guolei Xiang<sup>1\*</sup>, Tianyu Zhai<sup>1</sup>, Zikai Liu<sup>1</sup>, Weixin Zhao<sup>1</sup>, Xin Liang<sup>1</sup>, Leyu Wang<sup>1\*</sup>

1. State Key Laboratory of Chemical Resource Engineering, Beijing University of Chemical Technology, Beijing, 100029, P.R. China
2. State Key Laboratory of Coal Conversion, Institute of Coal Chemistry, Chinese Academy of Sciences, Taoyuan South Road 27, Taiyuan 030001, China

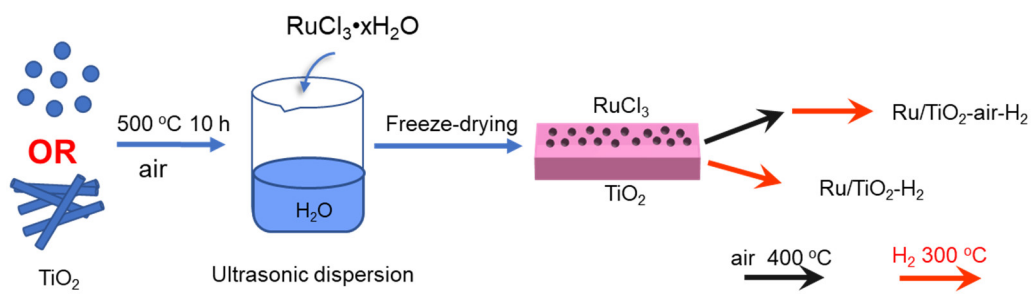
<sup>+</sup> These authors contributed equally

\*To whom correspondence should be addressed:

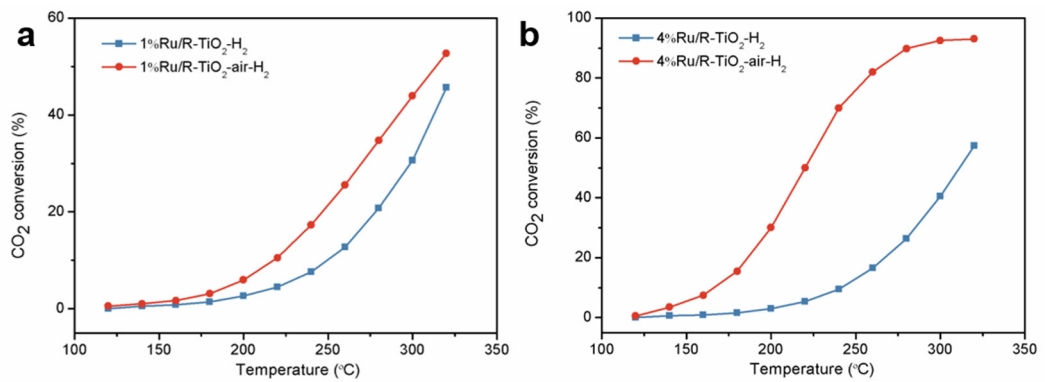
xianggl@mail.buct.edu.cn; (G. X.)  
lywang@mail.buct.edu.cn (L. W.)



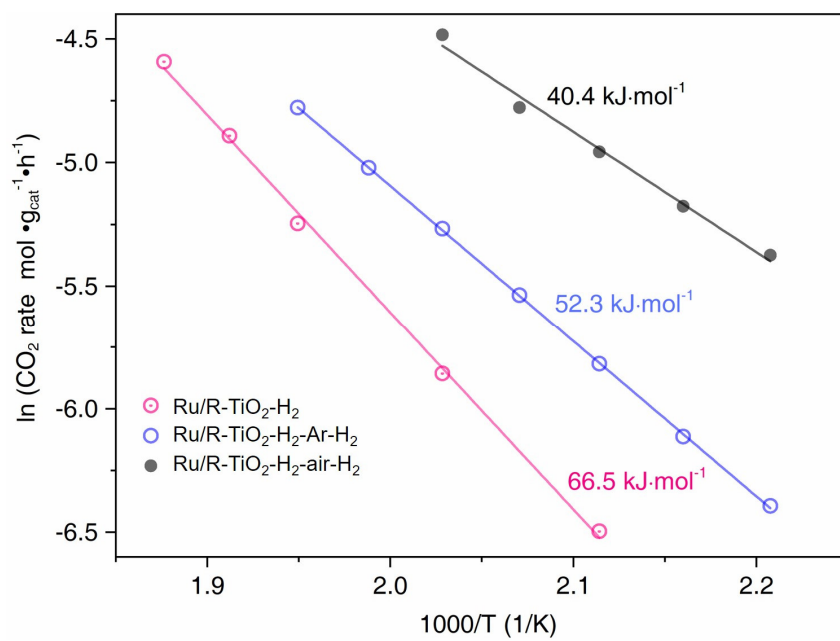
**Supplementary Figure 1.** TEM images of rutile- $\text{TiCl}_4$  (a), rutile- $\text{TiCl}_3$  (b), rutile-TiN (c) and anatase (d) after being annealed at 500 °C for 10 h.



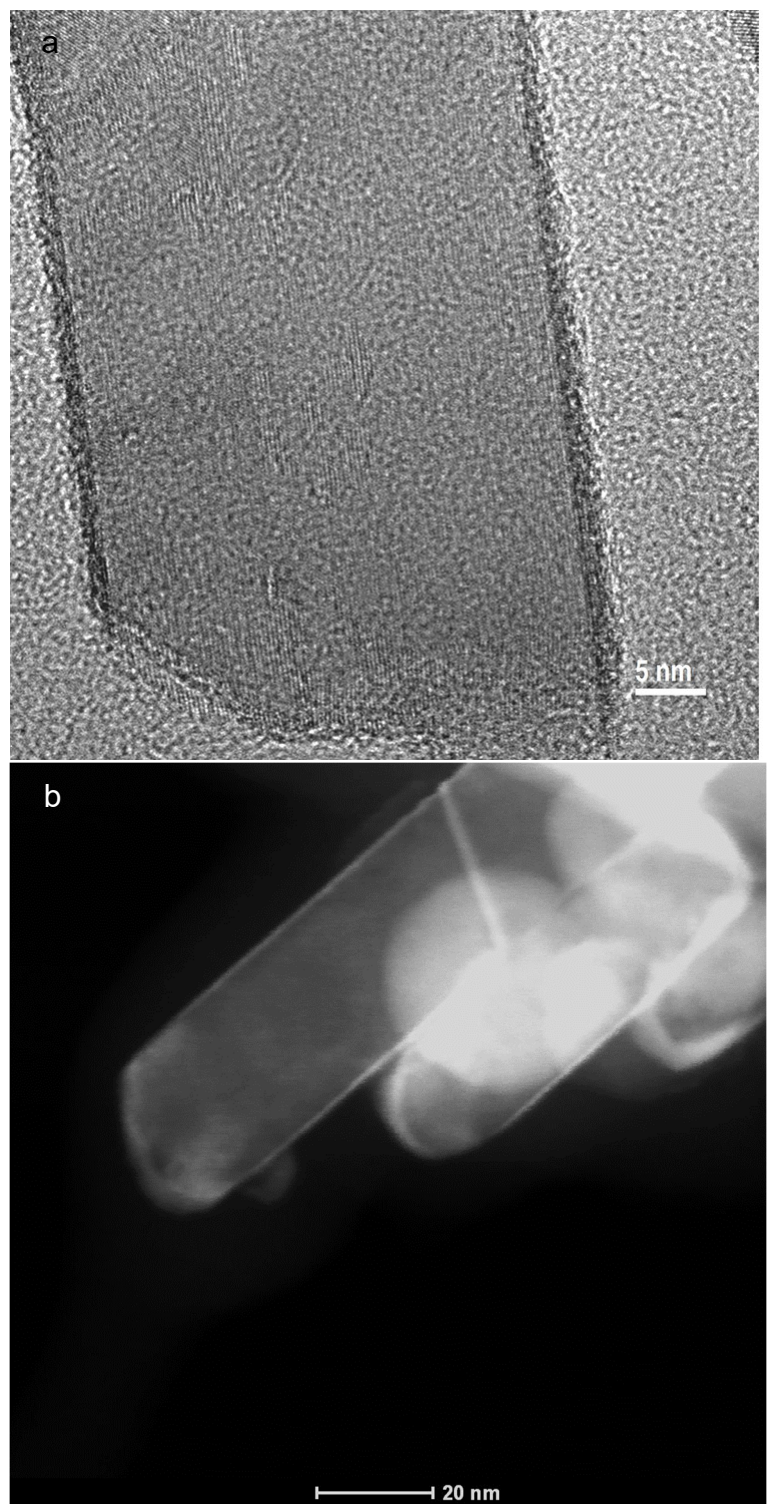
**Supplementary Figure 2.** Scheme of the synthetic procedures of  $\text{Ru/TiO}_2$  catalysts.



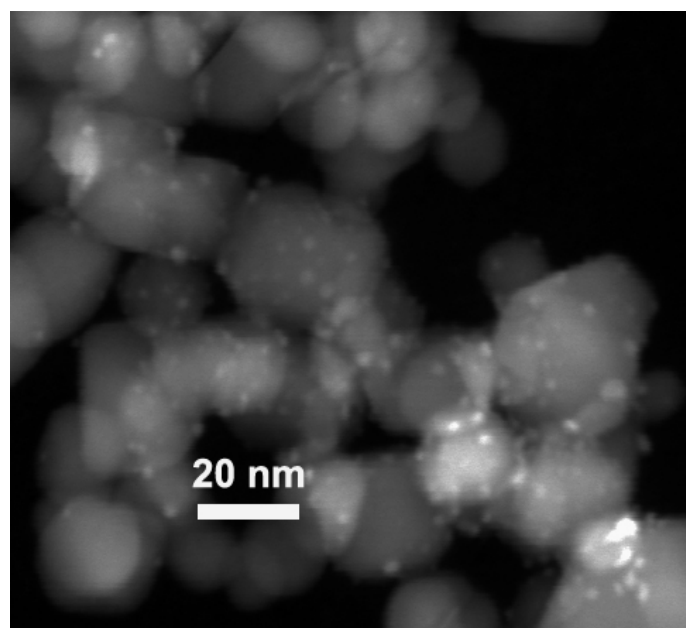
**Supplementary Figure 3.** Temperature-dependent CO<sub>2</sub> conversions of (a) 1%Ru/R-TiO<sub>2</sub> and (b) 4%Ru/R-TiO<sub>2</sub>.



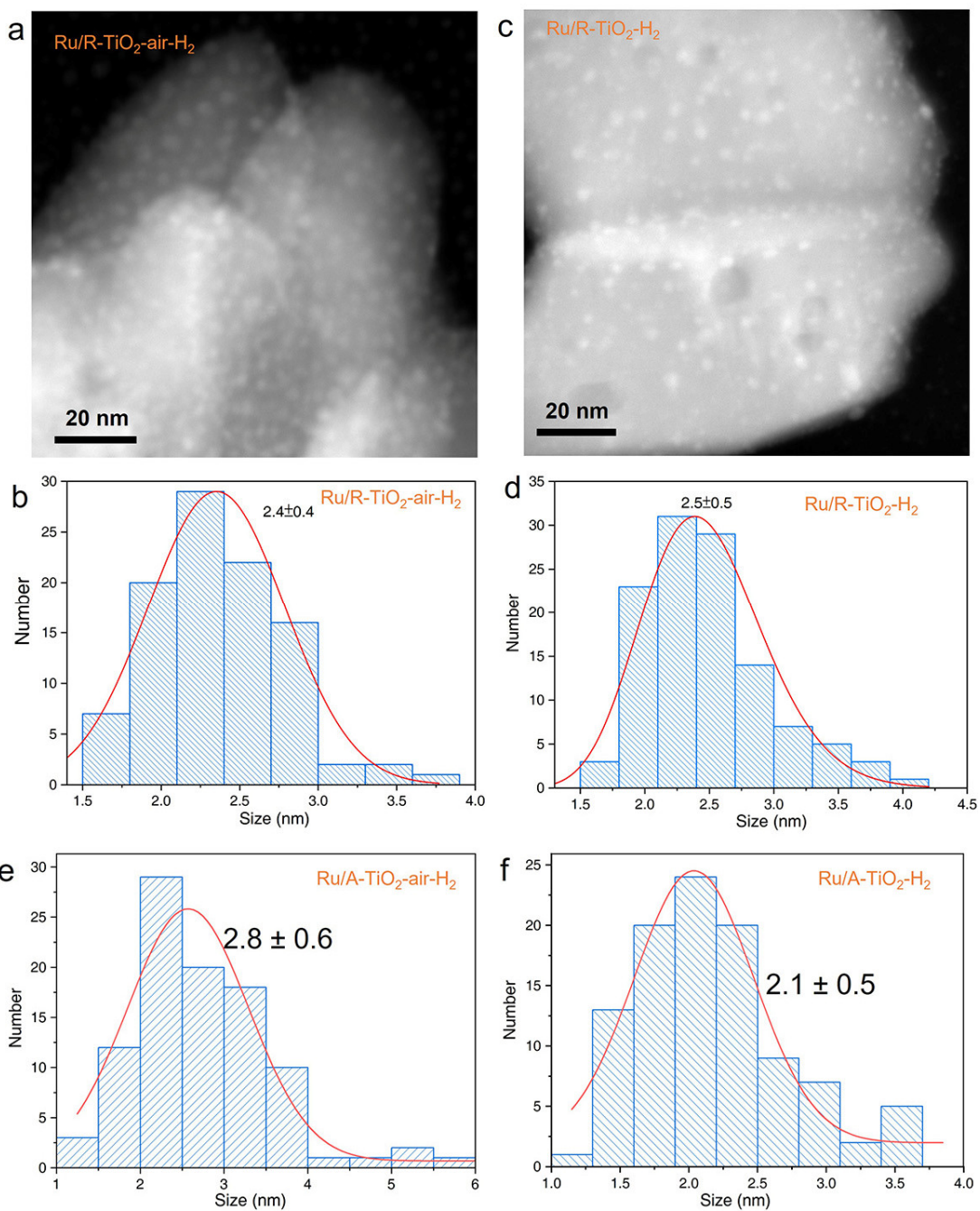
**Supplementary Figure 4.** Arrhenius plots of 2%Ru/R-TiO<sub>2</sub> catalysts treated in different procedures.



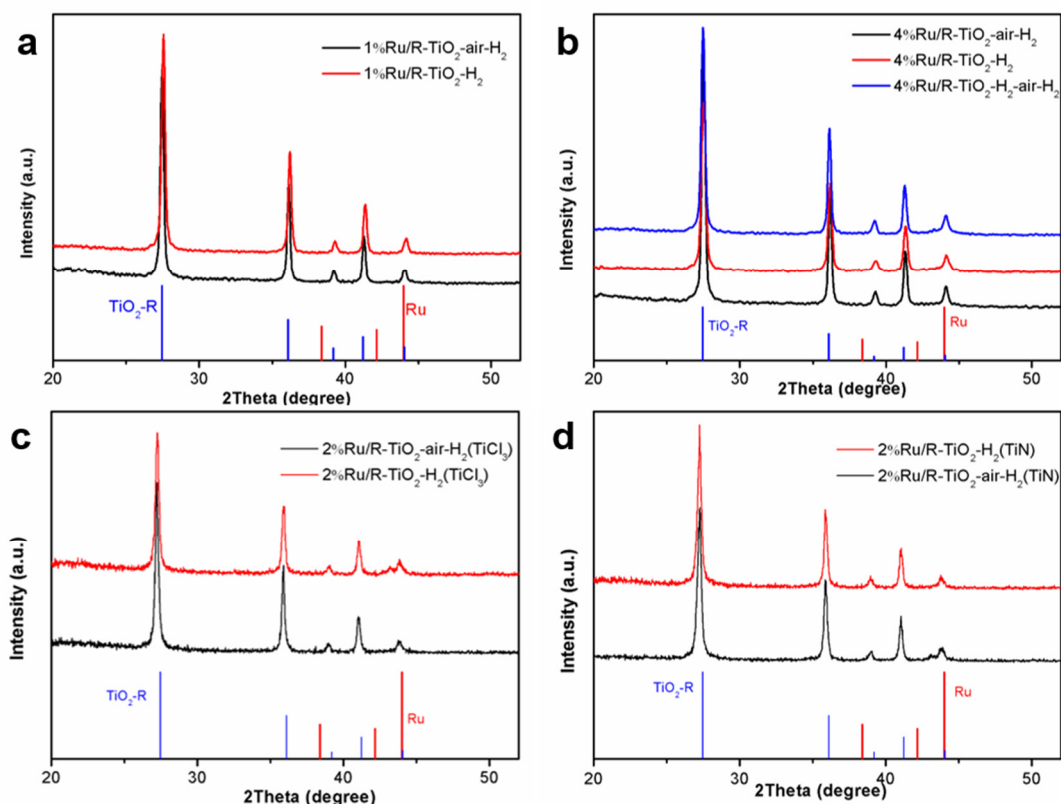
**Supplementary Figure 5.** TEM (a) and STEM (b) images of RuO<sub>2</sub> epitaxial layers on R-TiO<sub>2</sub> nanorod.



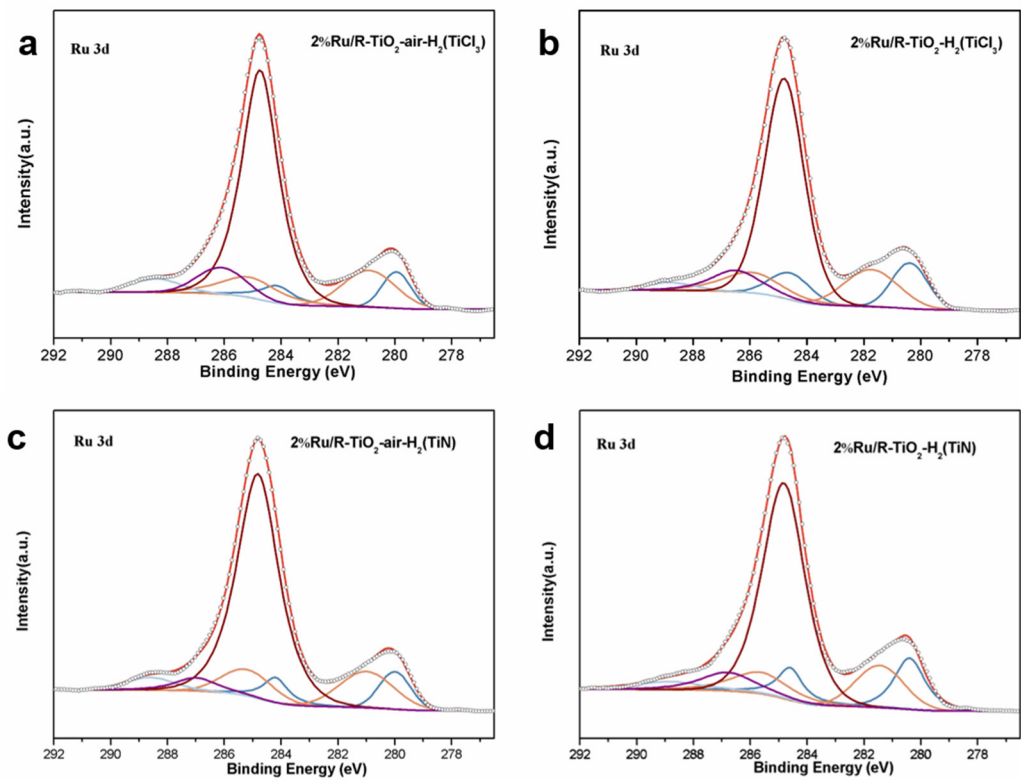
**Supplementary Figure 6.** STEM of RuO<sub>2</sub> on A-TiO<sub>2</sub>.



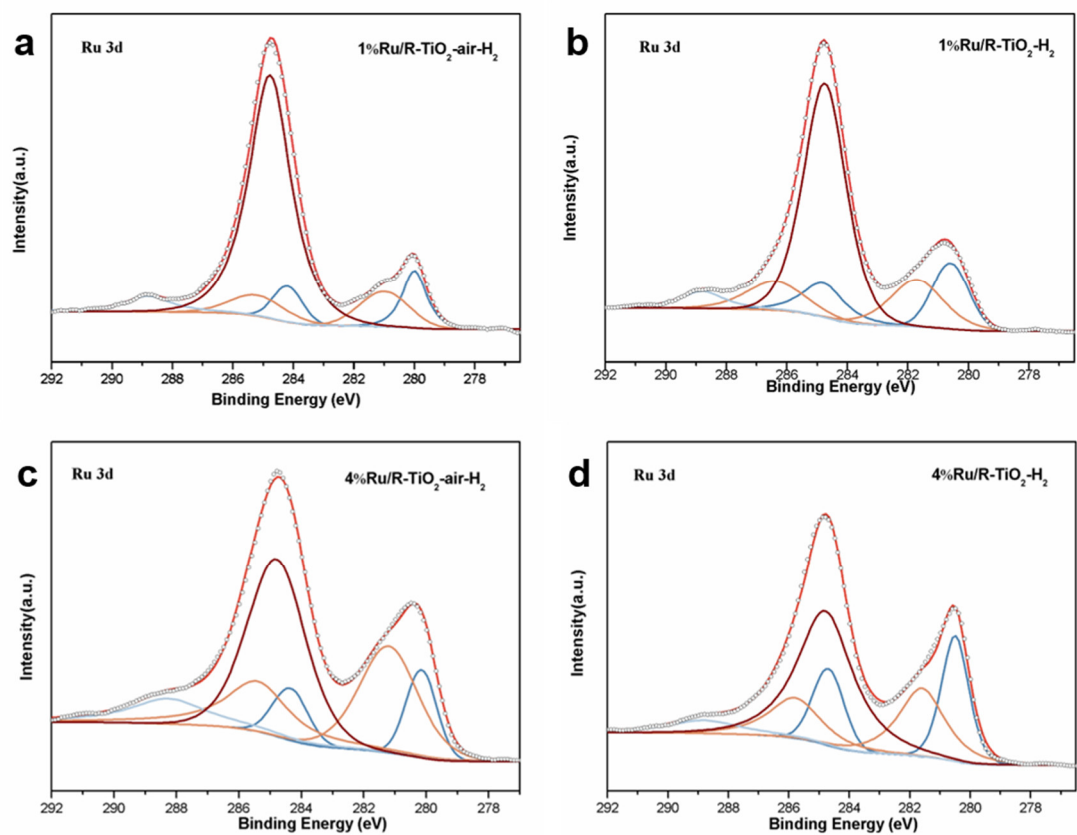
**Supplementary Figure 7.** Size distributions of 2%-Ru/TiO<sub>2</sub>-H<sub>2</sub> catalysts. STEM images of (a) Ru/R-TiO<sub>2</sub>-air-H<sub>2</sub> and (b) Ru/R-TiO<sub>2</sub>-H<sub>2</sub> catalysts. Size distributions of Ru nanoparticles of (c) Ru/R-TiO<sub>2</sub>-air-H<sub>2</sub>, (d) Ru/R-TiO<sub>2</sub>-H<sub>2</sub>, (e) Ru/A-TiO<sub>2</sub>-air-H<sub>2</sub>, and (f) Ru/A-TiO<sub>2</sub>-H<sub>2</sub> catalysts.



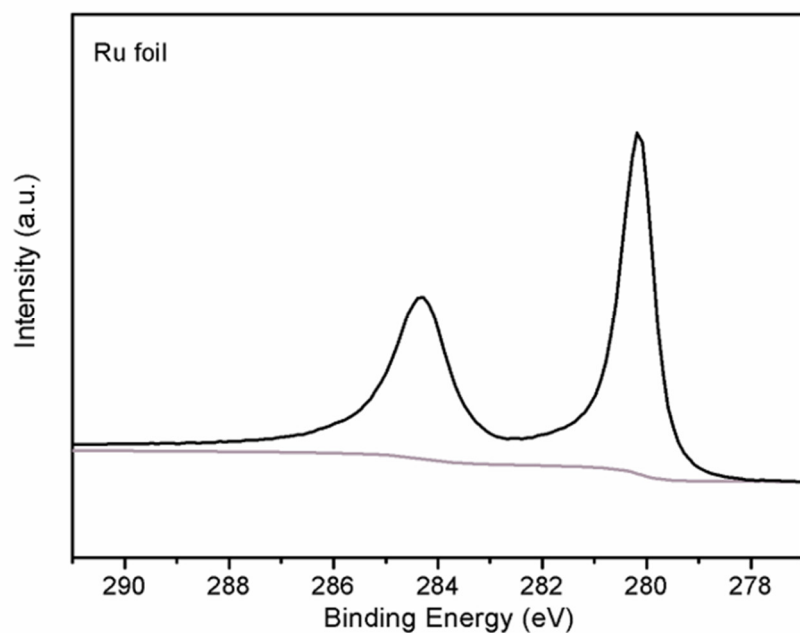
**Supplementary Figure 8.** XRD of 1%Ru/R-TiO<sub>2</sub> (a), 4%Ru/R-TiO<sub>2</sub>(b), 2%Ru/R-TiO<sub>2</sub>(TiCl<sub>3</sub>) (c) and 2%Ru/R-TiO<sub>2</sub>(TiN) (d) after reaction



**Supplementary Figure 9.** XPS of 2%Ru/R-TiO<sub>2</sub>-air-H<sub>2</sub>(TiCl<sub>3</sub>) (a), 2%Ru/R-TiO<sub>2</sub>-H<sub>2</sub>(TiCl<sub>3</sub>) (b), 2%Ru/R-TiO<sub>2</sub>-air-H<sub>2</sub>(TiN) (c) and 2%Ru/R-TiO<sub>2</sub>-H<sub>2</sub>(TiN) (d) after reaction.



**Supplementary Figure 10.** XPS of 1%Ru/R-TiO<sub>2</sub>-air-H<sub>2</sub>(a), 1%Ru/R-TiO<sub>2</sub>-H<sub>2</sub>(b), 4%Ru/R-TiO<sub>2</sub>-air-H<sub>2</sub>(c) and 4%Ru/R-TiO<sub>2</sub>-H<sub>2</sub>(d) after reaction.



**Supplementary Figure 11.** XPS of Ru foil.

**Supplementary Table 1. XPS fitting results of other catalysts.**

Sample	Binding Energy [eV]		The ratio of $\text{Ru}^{\delta+}/\text{Ru}^0$
	$\text{Ru}^{\delta+}$	$\text{Ru}^0$	
1%Ru/R-TiO <sub>2</sub> -air-H <sub>2</sub>	281.1	280.0	1.1
1%Ru/R-TiO <sub>2</sub> -H <sub>2</sub>	281.7	280.6	1.1
4%Ru/R-TiO <sub>2</sub> -air-H <sub>2</sub>	281.2	280.1	2.3
4%Ru/R-TiO <sub>2</sub> -H <sub>2</sub>	281.6	280.5	1.0
2%Ru/R-TiO <sub>2</sub> -air-H <sub>2</sub> (TiCl <sub>3</sub> )	281.1	280.0	1.8
2%Ru/R-TiO <sub>2</sub> -H <sub>2</sub> (TiCl <sub>3</sub> )	281.7	280.4	1.2
2%Ru/R-TiO <sub>2</sub> -air-H <sub>2</sub> (TiN)	280.9	279.9	1.9
2%Ru/R-TiO <sub>2</sub> -H <sub>2</sub> (TiN)	281.4	280.4	1.1

**Supplementary Table 2. Metal dispersion of Ru on rutile calculated by CO pulse adsorption**

Sample	Ru/R-TiO <sub>2</sub> -air-H <sub>2</sub>	Ru/R-TiO <sub>2</sub> -H <sub>2</sub>
D <sub>CO</sub> (%)	33.64	31.1